ELSEVIER

Marine Geology 192 (2002) 259–273

MARINE GEOLOGY
INTERNATIONAL JOURNAL OF MARINE GEOLOGY, GEOCHEMISTRY AND GEOPHYSICS

www.elsevier.com/locate/margeo

Migration history of a fine-grained abyssal sediment wave on the Bahama Outer Ridge

Roger D. Flood *, Liviu Giosan [1]

Marine Sciences Research Center, Stony Brook University, Stony Brook, NY 11794-5000, USA

Received 10 January 2001; received in revised form 3 March 2002; accepted 2 August 2002

Abstract

Abyssal mud waves (or fine-grained sediment waves) are often cited as evidence for deep current activity because subbottom profiles show that the wave form has migrated with time. The migration history of a fine-grained sediment wave on the Blake-Bahama Outer Ridge (ODP Site 1062) has been studied through the analysis of multiple ODP holes spaced across the wave. Additional information about wave migration patterns comes from 3.5-kHz records and watergun seismic profiles. These data suggest that wave migration has varied during the last ~10 Myr, although the only sediments sampled are younger than 4.8 Ma. Seismic profiles suggest wave migration was initiated about 8–10 Ma, and wave migration was pronounced from about 5 Ma to about 1 Ma (with an episode of wave reorganization about 4.5 Ma). Analysis of ODP cores suggests that migration rates have been somewhat lower and more variable during the last 1 Myr. Intervals of no wave migration are observed for several time intervals and appear to characterize deglaciations, especially during the last 500 kyr. Comparisons between seismic profiles and the core record show that most of the seismic horizons correlate closely with time horizons, and thus that the seismic profiles give a reasonable representation of sediment wave migration. Models suggest that wave migration is more pronounced during periods of higher bottom current flow and less pronounced during periods of lower current flow. Thus the migration record is consistent with generally higher bottom flow speeds at this site prior to 1 Ma and lower bottom flow speeds after 1 Ma. The Mid-Pleistocene Transition from a dominant climatic periodicity of 40 kyr to a dominant climatic periodicity of 100 kyr starts at about this time, suggesting an overall reduction in bottom flow speed at this site coincident with changing climate patterns. These changes in flow speed could be related to changes in the depth of the Western Boundary Undercurrent as well as to changes in the speed of thermohaline circulation.

Keywords: sediment wave; mud wave; furrow; abyssal circulation; Blake-Bahama Outer Ridge; paleocirculation; North Atlantic; Ocean Drilling Program; Mid-Pleistocene Transition; Site 1062

1. Introduction

Variations in North Atlantic Deep Water (NADW) production have been considered of major climatic importance due to the role this deep water mass plays in the intra- and interhemispheric heat and chemical exchanges (i.e. gases, salt,

[1] Present address: Department of Geology and Geophysics, MS#22, Woods Hole Oceanographic Institution, Woods Hole, MA 02543, USA.

* Corresponding author. Fax: +1-631-632-8820.

E-mail addresses: roger.flood@sunysb.edu (R.D. Flood), lgiosan@whoi.edu (L. Giosan).

0025-3227/02/$ – see front matter © 2002 Published by Elsevier Science B.V.
PII: S0025-3227(02)00558-3

nutrients; e.g. Broecker and Denton, 1989; Imbrie et al., 1992, 1993). Thermohaline overturn in the Nordic Seas via evaporative cooling of the warm, saline waters advected northward by the Gulf Stream perpetuates deep water formation by drawing additional warm waters to the north. In the North Atlantic, during warmer periods, NADW forms the lower part of the 'global ocean conveyor belt' (Broecker, 1991). This mode of thermohaline circulation can change dramatically during cold periods, with NADW production decreasing or coming to a halt (e.g. Alley et al., 1999 and references therein). At longer time scales, Raymo et al. (1990) studied the dynamics of the NADW production over the last 2.5 Myr by interpreting the deep ocean $\delta^{13}C$ gradients between Atlantic and Pacific. They found that glacial reductions in NADW were more intense in the Pleistocene than in the Late Pliocene. Bickert et al. (1997) confirmed this result, showing that glacial NADW production probably decreased after 1.6 Ma. This decrease was more severe in the last million years and particularly during the Mid-Pleistocene Transition period (~900–500 ka) when a change from a dominant climatic periodicity of 40 kyr to a dominant climate periodicity of 100 kyr occurred (Raymo et al., 1990, 1997; Bickert et al., 1997; Schmieder et al., 2000).

Deep water flow history can also be used to infer the dynamics of deep water mass production because the two are closely related. The carrier of NADW to the south along the eastern continental margin of North America is the Western Boundary Undercurrent (WBUC; Stahr and Sanford, 1999 and references therein), but at deeper depths the WBUC includes a component of Antarctic Bottom Water (AABW; Amos et al., 1971). Compositional and textural characteristics of sediments have been used to get direct information on past WBUC circulation (e.g. Hollister and Heezen, 1972; Barranco et al., 1989; Haskell, 1991; Bianchi et al., 2001; Giosan et al., 2002a,b). Abyssal mud waves (also called fine-grained sediment waves; Fig. 1) are often cited as evidence for deep current activity and they have been used to explore past deep flow variations (e.g. Manley and Flood, 1993; Brew and Mayer, 1998).

Fine-grained sediment waves appear to have developed in areas of abundant fine-grained sediment deposition where steady currents flow over the sea floor. Flood (1978, 1988) reported that internal waves in the water column were apparently fixed in position over sediment waves on the Bahama Outer Ridge (BOR) and suggested that a strong interaction was occurring at the present time. Sediment waves thought to be created by near-bottom flows are present on the levees of

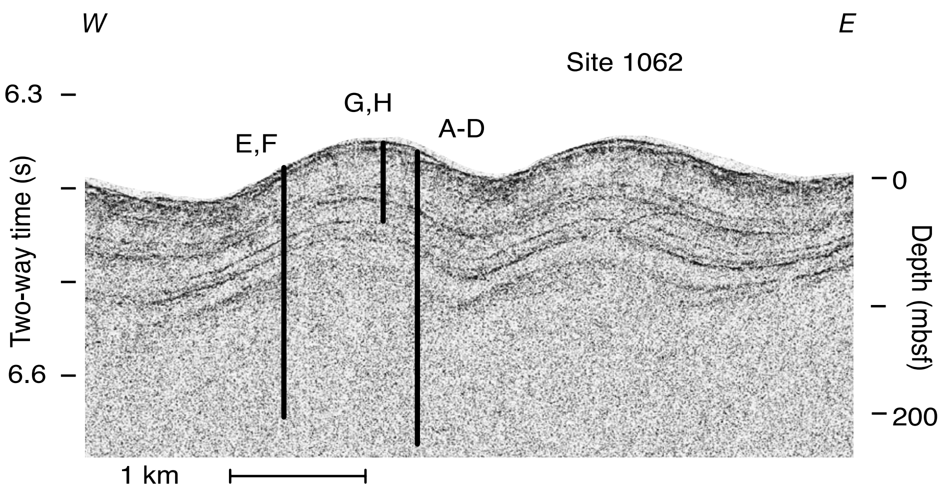

Fig. 1. 3.5-kHz subbottom profile collected across the fine-grained sediment wave site (ODP Site 1062). The locations of the three sets of holes drilled are shown. The locations of the holes and seismic line are shown in Fig. 4.

turbidity current channels as well as on sediment drifts (e.g. Normark et al., 1980). Normark et al. (1980) estimated a densiometric Froude number of about 1 for sediment waves on the Monterey Fan based on a two-layer flow model and they suggested that the sediment waves there are antidunes. However, there is no equivalent interface with a sharp density contrast in the deep ocean and thus Flood (1978, 1988) presented a conceptual model where internal waves developed on a density gradient rather than on a sharp interface. Flood (1978, 1988) reported that $\kappa = Nh/U$ (where N is the stability, h is the wave height and U is the free-stream velocity) ranged from 0.4 to 1.5 for sediment waves on the BOR. κ is the inverse of the gradient Froude number, indicating that the present-day Froude number for flow over these waves is about 1 and thus that these sediment waves can be described as antidunes. While a gradient Froude number of 1 indicates a strong interaction between flow and bedform, it does not provide insight into the precise mechanisms that leads to wave growth and migration. The lee-wave model presented by Flood (1978, 1988) does account for the upcurrent migration often observed for sediment waves (Fig. 2). While the model of Flood (1988) was developed for a bottom flow normal to the sediment wave crest, the general relationship between wave migration and flow

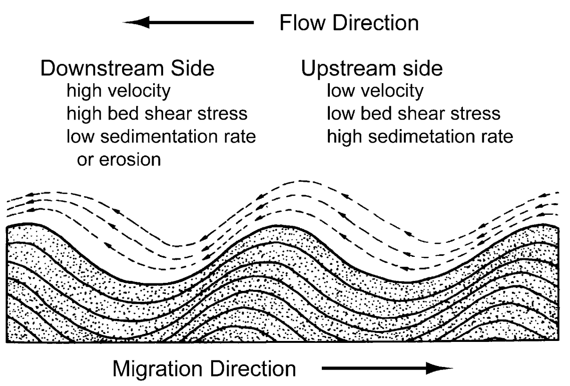

Fig. 2. The lee-wave model of sediment wave evolution showing the interaction of a flowing stratified water column flowing over the sediment wave profile. The flow slows as water climbs the upstream face of the wave and accelerates on the downstream face, resulting in enhanced deposition rates on the upstream side (after Flood, 1978, 1988).

over the wave appears to hold for most cases where sediment waves are at an angle to the mean current (Blumsack and Weatherly, 1989; Weatherly, 1993; Flood, 1994; Hopfauf et al., 2001). In the lee-wave model, a weakly stratified bottom flow is perturbed by the sediment topography leading to a change in the velocity structure of the flow. The flow decelerates on the upstream wave flank and accelerates on the downstream wave flank. The accumulation rate of fine-grained cohesive sediment decreases as shear stress increases (McCave and Swift, 1976), thus more sediment accumulates on the upstream wave flank where the flow speed is lower and the wave form migrates upstream. Enhanced wave migration is expected as flow speed increases because currents on the downcurrent flank approach the critical shear stress for deposition before those on the upcurrent flank (Flood, 1988).

Blumsack and Weatherly (1989) added a flow component parallel to the wave crest and noted that adding the along-wave flow can result in wave growth (higher accumulation rates on the wave crests), and that wave growth is necessary for waves to persist over time. They also suggested that along-wave flow can result in sediment wave migration at slow speeds when internal waves are not present. Zhang (1997) applied this model to determine sediment wave stability in different areas, including the waves studied by Flood et al. (1993) in the Argentine Basin. Hopfauf et al. (2001) extended the approach of Blumsack and Weatherly (1989) by taking into account the three-dimensional Coriolis vector. They suggest that downstream wave migration can occur at certain flow speeds if there is a poleward bottom flow component. However, they also indicate that downstream wave migration often occurs along with negative wave growth, suggesting that the waves will fill if these conditions persist for long periods.

While wave growth is necessary for long-term wave stability, it is the migrating character of the waves that is most noted on seismic profiles from sediment wave areas. The degree of wave migration can be most conveniently expressed as the ratio of sedimentation rates on the downstream to upstream sides (the sedimentation rate ratio, or SRR). Changes in cross-wave sedimentation patterns with time, as indicated by changes in SRR, are related through the lee-wave model to changes in the long-term average flow speed (Flood, 1988). The SRR will be less than 1 for a wave that has a component of upstream migration and greater than 1 for a wave that has a component of downstream migration. If individual sediment layers can be followed across a wave in the cores or seismic profiles, it is possible to construct a SRR record that can be used to examine the current regime history.

Wave migration can also be characterized in terms of the rate at which the wave shape moves across the sea floor (Wynn et al., 2000). The rate of lateral movement is directly related to the sedimentation rate, so information on both sedimentation rate and wave migration rate needs to be provided to characterize wave movement (e.g. Wynn et al., 2000). For a sinusoidal wave, a non-dimensionalized wave migration rate (WMR = wave migration rate/sedimentation rate or WMR = horizontal wave offset/vertical wave offset) can be related to SRR if the wave amplitude (B) and wavelength (L) are known because $\mathrm{WMR} \approx L/(2\pi B)(1-\mathrm{SRR})/(1+\mathrm{SRR})$.

In this study we employ core data, 3.5-kHz records, and watergun seismic profiles across a sediment wave on the BOR (Fig. 3) to examine the local flow history of WBUC over the last few million years. The sediment wave growth pattern can be interpreted to decipher past flow changes at various time scales. However, since only local flow variations are recorded by the sediment wave, additional data are necessary to distinguish between changes in current intensity (due to reductions in deep water production) and changes in position of the current axis relative to the investigated site.

2. Study area and background information

The flow of the WBUC along the eastern continental margin of North America has been responsible for the creation of a chain of sediment drifts (McCave and Tucholke, 1986). The BOR is a north–south sediment drift belonging to this chain, which extends as a continuation of the larger northwest–southeast trending Blake Outer Ridge (Fig. 3). Sediment drifts were initiated in the Oligocene when strong abyssal circulation began in the western North Atlantic (Miller and Tucholke, 1983). There is general agreement that the formation of NADW, the water mass that comprises most of the WBUC, was more or less continuous since Middle Miocene, some 10–12 Ma (e.g. Blanc et al., 1980).

At present WBUC flows to the south along the eastern flank of the BOR, makes a turn at the southern tip of the drift and continues to the north along the BOR's western flank (Fig. 3). It has been suggested that the overall deep circulation above the BOR may be more complicated than the presence of a single cyclonic gyre (Johns et al., 1997; Stahr and Sanford, 1999), but additional data are necessary to substantiate this hypothesis (Bianchi et al., 2001). Flow patterns may also have been different at times in the past. An extensive field of fine-grained sediment waves occurs on the west flank of the BOR at a depth of about 4750 m (Flood and Hollister, 1974; Flood, 1978; Laughton, 1981). It consists of waves oriented about NNE–SSW, about 35° to the regional contours which trend NNW–SSE (Fig. 4). Sediment wave heights range from 20 to 60 m and wavelengths from 2 to 2.5 km. The wave selected for drilling during ODP Leg 172 is 36 m high, has a wavelength of 2500 m, and is located at 28°14.75′N and 74°24.6′W at a depth of 4723 m. Short-term current-meter measurements and bottom photographs show that bottom currents in the study area are remarkably stable and flow along the regional contours to the north-northwest with speeds up to about 10 cm/s (Flood and Hollister, 1974; Hollister et al., 1974). The core of the WBUC, where average speeds of 20–40 cm/s have been recorded (Jenkins and Rhines, 1980), is positioned higher than the BOR at about 4100 m depth. At the depth of the sediment wave study site on the western flank of the BOR the present-day WBUC is a mixture of NADW and AABW, containing about 15% AABW (Amos et al., 1971).

ODP Leg 172 drilled eight holes into the selected wave: Holes 1062A, 1062B, 1062C and

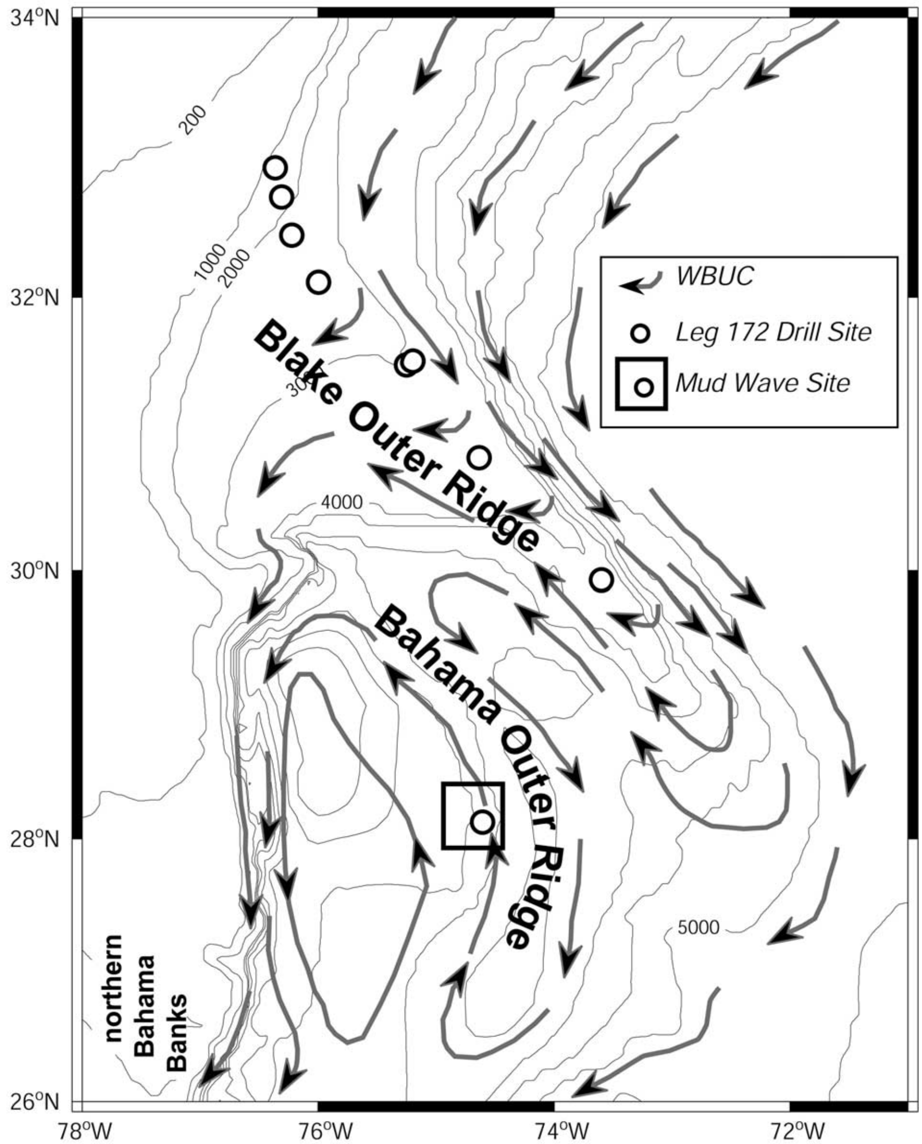

Fig. 3. Map of the Blake-Bahama Outer Ridge showing the stream lines of bottom flow and the location of the study site at ODP Site 1062 (Fig. 4). Isobaths are in m. Bottom flow directions at the sediment wave site are towards the north-northwest.

1062D are on the east (upcurrent and upslope) flank of the sediment wave; Holes 1062E and 1062F are on the west (downcurrent and downslope) flank; and Holes 1062G and 1062H are on the wave crest (Figs. 1 and 5). Shipboard biostratigraphic analyses suggest that sediments somewhat older than middle Pliocene ($>$2.83 Ma) were recovered on the west flank while on the east flank the deepest hole penetrated into early Pliocene ($>$4.27 Ma). Because of wave migration, holes on the east flank of the modern wave sample sediments from the west flank of buried waves that are at subbottom depths of more than about 150–175 m, and vice versa. Overall, the sedimentary sequences recovered from the two wave flanks are similar (Keigwin et al., 1998). They

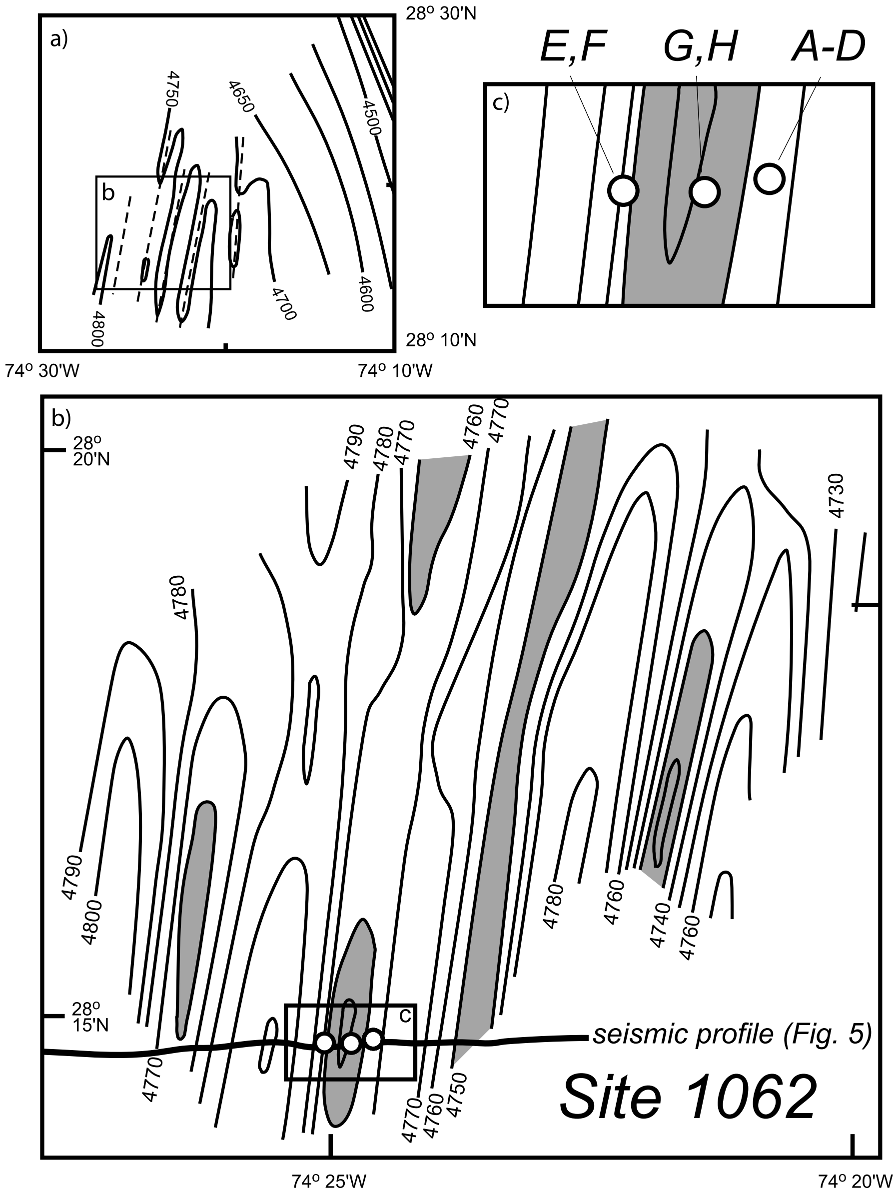

Fig. 4. Index map of Site 1062 showing (a) the wave orientation patterns (crests are dashed lines), (b) the site bathymetry and location of the seismic profile shown in Fig. 5, and (c) the location of the drill holes with respect to the wave. The wave crests are oriented north-northeast while bottom flow directions are towards the north-northwest (Fig. 3). Bathymetry in m after Flood and Hollister (1974) and Flood (1978), wave crests are shaded. For location, see Fig. 3.

consist of an alternation of nannofossil-rich and clay-rich sediments forming Unit I that extends from the present to Stage 16 (an age of about 625 ka, at subbottom depths of about 75 m), followed by the clay-rich Unit II (subbottom depths of 75–165 m) and the mixed-sediment Unit III (subbottom depths of 165 to over 240 m). The boundary between the last two units is ~2.7 Ma.

Units II and III contain thin distal aragonitic turbidites originating from the Bahama Banks

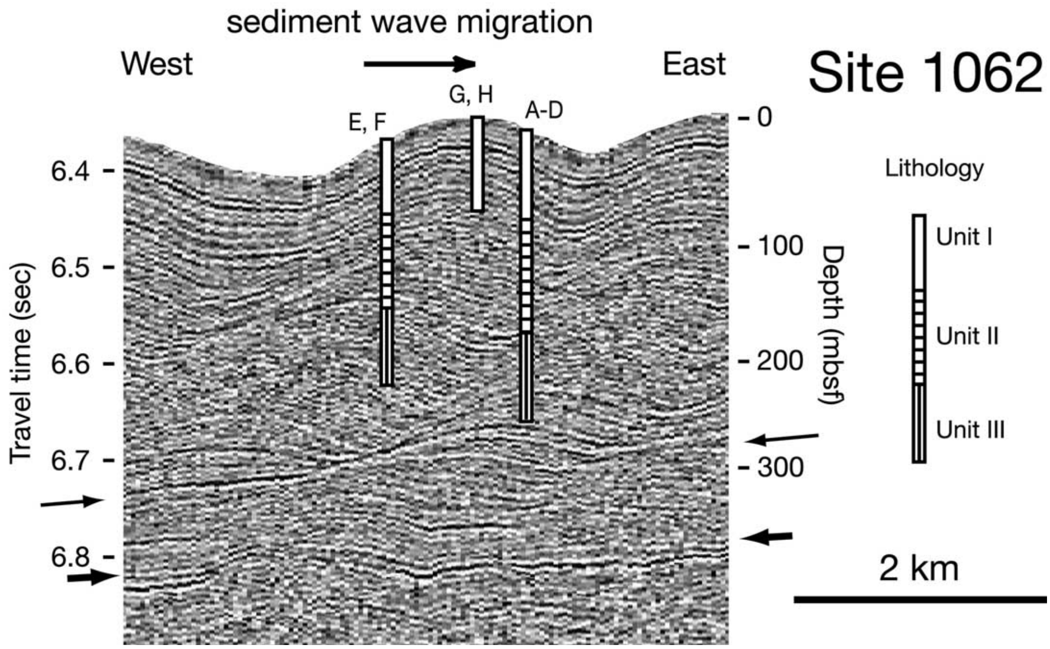

Fig. 5. Watergun seismic profile collected at the sediment wave site showing locations of holes and the lithologic units at Site 1062. The location of the profile is shown in Fig. 4. Longer arrows on either side of the profile at about 6.7 s (~300 m) indicate a possible wave reorganization event and bold arrows on either side of the profile at about 6.8 s mark the base of the sediment waves.

(Keigwin et al., 1998) which make up less than 1% of the sediment record. Seven aragonitic turbidites, with an average thickness of about 10 cm, are in the 90-m-thick Unit II (from about 600 ka to 2 Ma) and 12 thinner turbidites are in Unit III (older than about 2 Ma); however, the few turbidites that appear to correlate across the sediment wave are generally thicker on the southeast wave flank suggesting that the turbidite record has also been affected by wave morphology (Keigwin et al., 1998). Keigwin et al. (1998) suggest that these turbidites have a source on the Bahama Banks about 300 km to the southwest (Fig. 3), although there is no indication of a turbidite pathway, channel or levee in seismic profiles on the BOR. Flood (1978) described a similar aragonitic layer at about 100 kyr in piston cores over 100 km apart from the west flank of the BOR. The apparent large areal distribution of the turbidites and the lack of any channel morphology suggest that they were formed by large but rare turbidity currents from the Bahama Banks or Blake Escarpment that traveled throughout the basin. There is at present no indication that the turbidity current events played a role in the formation or evolution of these sediment waves.

3. Results and discussion

We recovered a 900 000-year record of the SRR at Site 1062 through detailed correlation of layers between the upstream and downstream wave flanks. This corresponds to the upper ~85 m of sedimentary section which is the interval where a continuous, overlapping sediment sequence was recovered on both wave flanks. Primary evidence for the cross-wave changes in accumulation rates that result in wave migration comes from biostratigraphic and magnetostratigraphic analysis (Keigwin et al., 1998). For example, using the last occurrence of the deepest common biostratigraphic datum (top *Discoaster pentaradiatum* at 2.52 Ma), sedimentation rates were found to be 25% higher on the eastern flank than on the western flank. At a finer scale, the spliced physical properties and color records from the east wave flank, wave crest, and west wave flank show remarkable similarity to one another and individual features can in general be correlated across the wave (Fig. 6; Keigwin et al., 1998).

The time scale for this record is based on an orbitally tuned age model (Grützner et al., 2002) developed using the predicted carbonate records of Giosan et al. (2001) and the shipboard composite stratigraphic sections at each site (different composite sections were made for the two wave flanks; Keigwin et al., 1998). The phasing between the orbital curves and carbonate records for all Leg 172 sites was adjusted using available oxygen isotope data from older cores in the region as well as on Leg 172 cores (Grützner et al., 2002). We anticipate a revised age model as more isotopic data become available from Leg 172 cores. Possible errors are introduced into the age model by uncertainty in correlation between holes, errors in vertical positioning, and distortion during coring and after core retrieval (Hagelberg et al., 1991). Age datums are about 10–15 kyr apart during the last 500 kyr and about 20–30 kyr apart from 500 to 900 kyr.

3.1. Core record

A robust record of sedimentation rates for each wave flank was constructed from the ODP cores based on correlating individual cores to the model of Grützner et al. (2002). Records of predicted carbonate, measured magnetic susceptibility and the two parameters resulting from the sediment

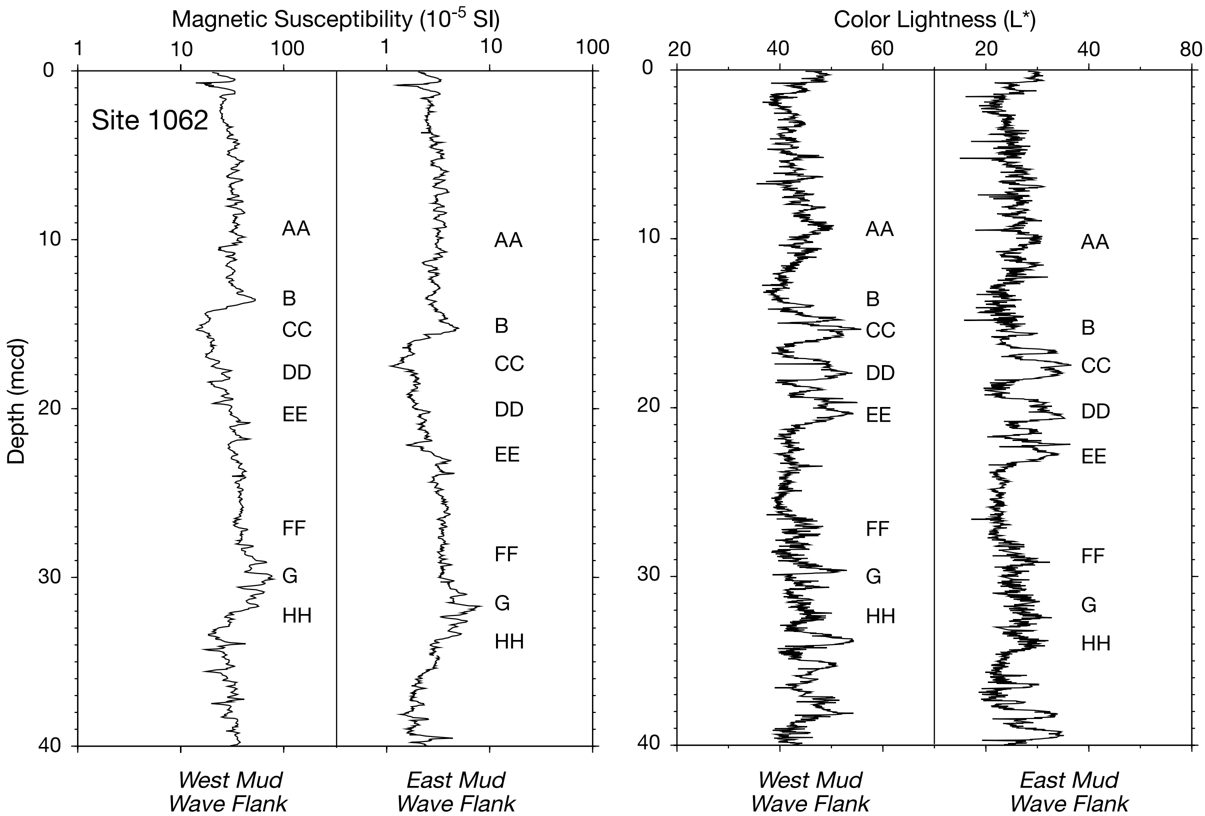

Fig. 6. High-resolution down-core records of magnetic susceptibility (left) and color lightness (right) demonstrating the high degree of correlation between the west and east core flanks. Features marked B and G are correlated based on color lightness while features marked AA, CC, DD, EE, FF, and HH are correlated based on magnetic susceptibility (mcd = meters composite depth; after Keigwin et al., 1998).

reflectance factor analysis (Giosan et al., 2001) were used for this correlation. Composite depths for each time horizon were adjusted for each core in a hole on one wave flank by correlating the four variables in each core with the spliced record. We used the program ANALYSERIES (Paillard et al., 1996) to determine the degree of stretching or squeezing needed for optimal correlation between the identified time horizons in each core and the spliced record. As a result of this procedure, coeval layers from all holes at a site were arranged on the same depth scale. Sedimentation rates were then calculated for each hole as well as for the spliced record for each wave flank (Fig. 7, upper). Sedimentation rate ratios were computed for each pair of holes situated on opposite wave flanks, resulting in up to eight values for the SRR between each set of dated horizons. Comparison of the maximum, minimum and mean SRR values with age shows a limited range of variation suggesting that this general pattern is not overly affected by inaccuracies introduced by (1) natural inter-hole variability in sedimentation, (2) uncertainty in vertical positioning or (3) core distortion. Fig. 7 (lower) shows the mean of the SRRs calculated for each level.

Sedimentation rates on both flanks of the sediment wave have steadily increased over the last 400 kyr with significant maxima for the last three glacial periods (Fig. 7). This is a generalized phenomenon for all Leg 172 sites in water depths below $\sim$3000 m, and it was attributed by Giosan et al. (2002a) to a possible reinvigoration of the NADW production since Stage 11 (Raymo et al., 1990). The enhanced NADW may have led to a stronger WBUC at depths below 3000 m, bringing more sediment to the Blake-Bahama Outer Ridge. There also may have been more sediment available basinwide since Stage 6 due to an intensified glacial erosion and delivery from the Laurentian Ice Sheet (Giosan et al., 2002a).

The SRR determined from the cores is generally under 1 for the last 900 kyr, averaging about 0.75 with minimum values of about 0.5 and maximum values of about 2.3. Younger than about 400–500 ka (i.e. younger than Stage 11) SRR values are consistently low, and the few intervals of increased SRR appear to be restricted to late glacials and early interglacials. For example, SRR $>$ 1 is found from mid-Stage 6 to mid-Stage 5 and less pronounced increases are observed at other glacial–interglacial transitions (e.g. 8–7 (weak), 10–9, 12–11 (weak)). The SRR pattern in sediments older than about 400–500 ka is somewhat different from that in younger sediments with more intervals of SRR values near or over 1, including two extended intervals with SRR greater than 1.5 (in Stages 21 and 13).

We can interpret this record in terms of bottom flow speed by linking intervals of lower SRR to periods of faster (or perhaps steadier) current flow and intervals of higher SRR (near 1) to periods of slower (or perhaps less steady) current flow. The intervals of SRR $>$ 1 could result from errors in correlation or from distortion in coring, especially deeper in the core where SRR $>$ 1 often correlates with a low sedimentation rate. Alternatively, the intervals of SRR $>$ 1 could represent periods of downstream wave migration as predicted by Hopfauf et al. (2001) for a poleward bottom flow, or they could represent periods when the overall circulation pattern was different from that observed today. The generally low sedimentation rate when SRR $>$ 1 suggests a preliminary interpretation that these intervals mark times of low flow. Thus the SRR record at Site 1062 suggests that a current has been active at this site for much of this record with some periods of weak flow. This SRR pattern indicates stronger bottom currents during late interglacials and early glacials, and reduced flow (or perhaps less steady flow) during late glacials and early interglacials, especially later than about 400–500 ka. This is consistent with a reduced production of NADW during meltwater episodes characterizing deglaciations (see e.g. Keigwin et al., 1998, for a review on NADW circulation modes). The occasional low SRR values in Unit II and the early part of Unit I (i.e. earlier than about 400–500 ka) also suggest periods of faster bottom current flow.

Hole 1062E recovered a sequence of inclined bedding in Core 5H, (about 240–290 ka) that was interpreted as furrow fill. If the furrow was being filled in an interval of no current, one might expect that the sedimentation rate on the west flank at this time (from about 190 to 340 ka)

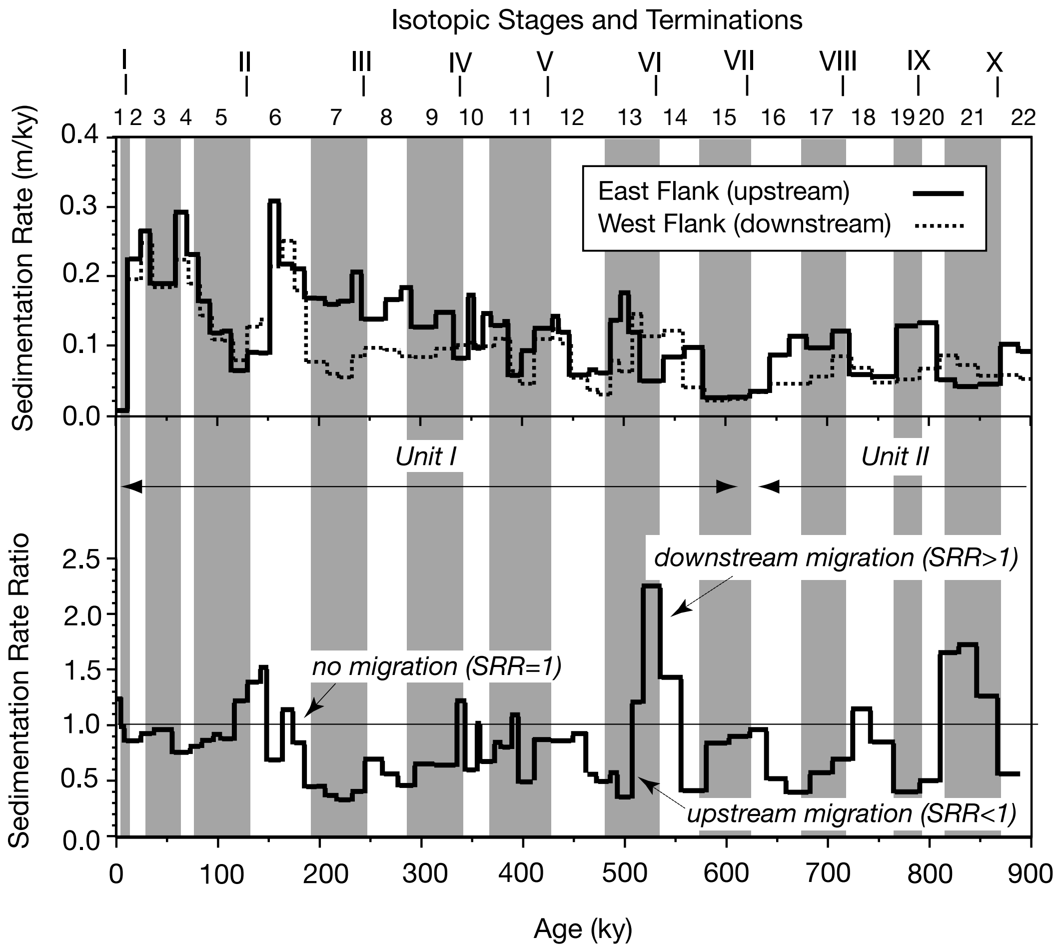

Fig. 7. Sedimentation rates (upper) and SRR (lower) at the sediment wave study site as determined through analysis of cores collected at Site 1062.

would be higher than on the eastern wave flank where no furrow is indicated. However, the sedimentation rate on the western flank is actually lower than on the eastern flank (SRR ≈ 0.6). This suggests that the furrow most likely existed in a time of higher current flow, consistent with a low SRR. The apparent increase in SRR at the Stage 8–7 boundary could have been reduced by sedimentation patterns related to the furrow.

3.2. Seismic record

Watergun seismic and 3.5-kHz profiles were studied to determine to what extent the migration pattern identified on profiles agrees with that determined from the drill holes. The watergun seismic record (Fig. 5) was collected during R/V *JOIDES Resolution* Leg 172 using a 80 cu. in. generator–injector gun and was digitized at 1 ms. The 3.5-kHz profile (Fig. 1) was collected on R/V *Knorr* Cruise 140-2 and was digitized at 12 kHz. Initial processing of the watergun seismic profile is described in Keigwin et al. (1998), and the profiles are displayed as gray-scale images. These profiles show that several of the individual reflections can be traced across the wave (Fig. 8, Table 1). However, other reflections are difficult to trace across the wave, especially deeper in the section. Correlating between the seismic profiles and the cored sediment age requires two steps. First, trav-

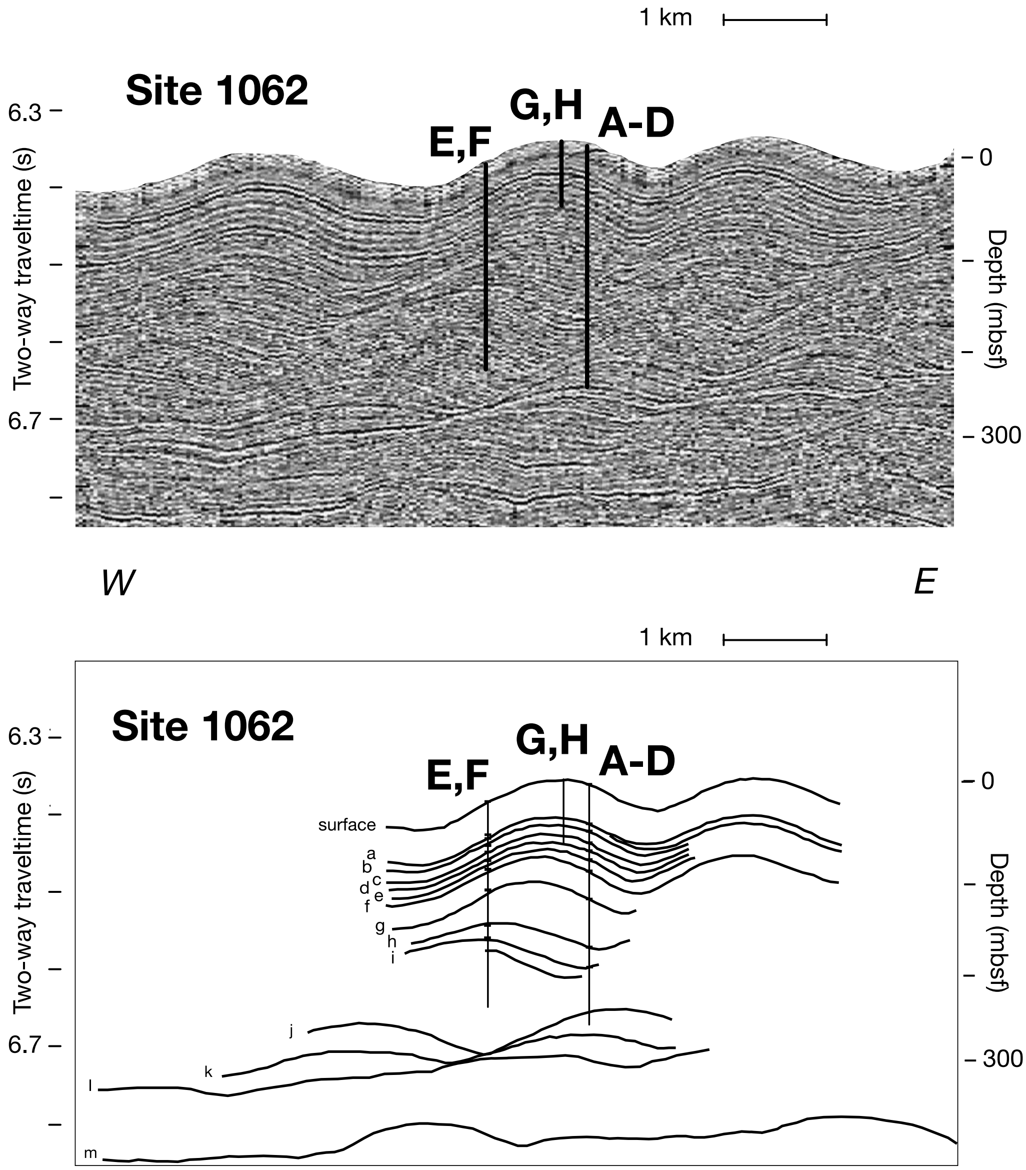

Fig. 8. Watergun seismic profile (upper) and traced reflections (lower) of the fine-grained sediment wave. The marks labelled a–i indicate the same sediment age on both wave flanks. The marks generally fall within a few milliseconds of the traced reflection on the western wave flank, suggesting that the seismic reflections accurately portray fine-grained sediment wave evolution. Reflections j, k, l and m mark significant events in wave evolution. For location see Fig. 4.

el time on the seismic profile needs to be converted to subbottom depth using an appropriate sound velocity profile, and second, subbottom depth at the core site needs to be converted to composite depth on the spliced record. The depth, lithology and age in each hole can be determined from the composite depth. The sediment velocity profile was determined for this site based on downhole velocity logs at other Leg 172 sites (Sites 1061 and 1063) and from bulk density and P-wave data collected on discrete samples and with the MST (multisensor track) at Site 1062 following the approach of Flood et al. (1997). This analysis suggests that sediment velocity increases linearly from about 1440 m/s at the sediment surface to about 1660 m/s at 300 m below sea floor, and thus depth in the sediment can be estimated from travel time by d (m) = (1440 tt)/(2−0.733 tt), where tt is the two-way travel time in seconds. Depth in the sediment determined from the seismic profile can be related to the composite depth scale by fitting a curve to measured depth vs. composite depth for each core top in a composite. Different curves are needed for different depth intervals because the degree of core expansion changes down-core, especially at the change from APC to XCB coring.

Nine seismic reflections, labeled a–i from the youngest to the oldest (from about 225 ka to 2.6 Ma), were traced across the sediment wave (Fig. 8, Table 1). Reflections down to g are traceable in both 3.5-kHz and watergun seismic records while h and i are recognized only in the watergun seismic record. It was not possible to trace reflections below i between drill sites on the two wave flanks. The ages of the seismic reflections were determined on both wave flanks through correlation between the seismic profile and the cores, and the ages were then compared. The ages of seismic reflections on the western wave flank are usually 50 kyr (range 35–85 kyr) older than the ages of the same reflections on the eastern wave flank. These age differences correspond to depth differences of about 5 m (range 3.5–8.5 m) for an average sedimentation rate of 0.1 m/kyr or a travel time difference of 6.5 ms (range 4.5–11.3 ms). This mismatch could occur through an error in correlating from the seismic profiles to the composite core. It could also occur because seismic reflections do not always correspond to age horizons in the core, and because some of the reflections are difficult to follow over the wave unambiguously. Mayer (1979a,b) and others have suggested that closely spaced lithologic boundaries can create spurious reflections on seismic and 3.5-kHz profiles.

There are several clear reflections on the 3.5-kHz record, especially from about 30 to 75 m, in the zone of pronounced reflections on the watergun seismic record. Reflections are less distinct in the upper 30 m except for a reflection at about 5 m, and most of the reflections, including the sediment–water interface, have hyperbolic echoes superimposed on them that indicate the presence of furrows across the sediment wave profile (Flood and Hollister, 1974; Tucholke, 1979; Flood, 1980). The migration pattern observed on the 3.5-kHz record extends to about 0.12 s (90 m) subbottom, and reflections in the 3.5-kHz records are indeed more closely spaced on the western flank than on the eastern flank, evidence that the wave has migrated to the east-southeast (upcurrent and upslope, Figs. 1 and 4). The wave has migrated laterally about 125 m in the upper 66 m (horizontal migration rate about 0.37 m/kyr; sed-

Table 1
Sediment wave layer summary

Seismic reflection	Age (kyr)	Holes 1062A–D		Holes 1062E–F		
		Two-way travel time (ms)	Subbottom depth (m)	Two-way travel time (ms)	Subbottom depth (m)	SRR at wave flank
Surface	0	0	0	0	0	
a	225	50	37	45	33	0.90
b	279	60	44	53	39	0.83
c	358	74	55	63	46	0.68
d	440	84	62	72	53	0.89
e	513	96	71	80	59	0.69
f	672	110	82	89	66	0.62
g	999	145	110	116	87	0.75
h	2214	206	160	153	117	0.31
i	2661	231	181	174	134	0.26

imentation rate about 19.4 cm/kyr; SRR about 0.82; WMR about 1.9).

The watergun seismic record shows the wave structure to about 0.45 s two-way travel time (400 m below sea floor; bold arrows in Fig. 5 and reflection m in Fig. 8) and shows at least one distinct change in wave migration pattern. From about 0.45 to 0.35 s (400 to 300 m) subbottom (between reflections m and l in Fig. 8) the waves are somewhat irregular in form and there is little migration (SRR near 1; WMR near 0). Above that interval the waves become more regular and migration becomes more pronounced to about 0.15 s (76 m) subbottom (reflection g on Fig. 8). An average SRR for the interval from 2.05 Ma to 1.15 Ma is 0.36, WMR is 10.4, the wave migration rate is 1.04 m/kyr and the sedimentation rate is 10 cm/kyr. The seismic reflections become stronger above about 0.15 s (76 m) and the migration is less and consistent with that observed on the 3.5-kHz record. Overall the waves have migrated horizontally about 2000 m over the 0.45-s (400-m) wave record, with most of that migration occurring between 0.35 and 0.15 s (300 and 76 m) subbottom. The interval of pronounced migration (0.35–0.15 s; 300–76 m subbottom) is interrupted at about 0.30 s (215 m) by an undulating reflection (reflection k in Fig. 8) that appears to erode the underlying waves, although the waves reorganize and re-grow above this horizon. Extrapolating sedimentation rates at Site 1062 suggests an age of about 8–10 Myr for the initiation of the wave field, an age of 5 Myr for the increase in migration rate, and an age of 4.5 Myr for the wave reorganization event. The zone of near-surface waves with lower migration (shallower than about 90 m) correlates to the last 1 Myr.

The SRR values determined from the 3.5-kHz records and the watergun seismic profiles are quite similar to the average values determined for this time interval by drilling (SRR $\approx$ 0.75), although the seismic record is not able to resolve the smaller changes in SRR noted in the cores. This agreement is encouraging and suggests that the trends observed in both 3.5-kHz and seismic records are likely to be real and can be used in interpreting the wave migration pattern. The migration pattern suggests that flow was stronger before 1 Ma than after, which is consistent with a higher NADW production before the Mid-Pliocene Transition at ~0.9 Ma (Raymo et al., 1990, 1997; Bickert et al., 1997).

4. Conclusions

This study suggests that a record of sediment wave migration preserved in cores and in seismic profiles provides important insights into the history and character of bottom current flow at this site. The core record can be interpreted to give SRR values every 10–15 kyr. More detailed correlation is possible between cores, but the number of age datums presently available limits the resolution of the SRR record. A consistent but lower-resolution record is derived from analysis of seismic profiles, although apparently continuous reflections cannot be unambiguously correlated between holes on seismic profiles.

Intervals of reduced or no wave migration (observed in cores) are noted for several time intervals on the BOR, and they appear to characterize deglaciations. Over longer time scales (observed in seismic profiles), the wave was migrating faster from about 4 to 1 Ma suggesting a stronger bottom flow at that time and a reduction in bottom flow at about 1 Ma. This would be consistent with a decrease in NADW production detected in $\delta^{13}C$ deep water evolution recorded by benthic foraminifers and a less vigorous ocean circulation (Raymo et al., 1990; Bickert et al., 1997).

While we appear to be detecting changes in bottom flow speed by studying sediment wave migration, we cannot determine from the wave motions alone which water masses are responsible for the reduction or increase in flow speed. For example, additional information is needed to determine to what extent flow changes at this site were caused by changes in ocean circulation or by vertical migration of the WBUC. This illustrates the fact that a fine-grained sediment wave is a fixed recorder of the flow, and therefore cannot distinguish between flow variations due to changes in deep water production or due to a repositioning of a deep current relative to the wave.

Acknowledgements

This research used samples and data provided by the Ocean Drilling Program (ODP). The ODP is sponsored by the U.S. National Science Foundation (NSF) and participating countries under management of Joint Oceanographic Institutions (JOI), Inc. Funding for our participation in Leg 172 and our post-cruise studies was provided by the U.S. Science Support Program Grants USSSP168 and F000562. Reviews by J.C. Faugères, R.B. Wynn and A. Akhmetzhanov are gratefully acknowledged. This paper is contribution number 1237 of the Marine Sciences Research Center of Stony Brook University.

References

Alley, R.B., Clark, P.U., Keigwin, L.D., Webb, R.S., 1999. Making sense of millennial-scale climate change, In: Clark, P.U., Webb, R.S., Keigwin, L.D. (Eds.), Mechanisms of Global Climate Change at Millennial Time Scales. AGU Geophys. Monogr. 112, 385–494.

Amos, A., Gordon, A., Schneider, E.D., 1971. Water masses and circulation patterns in the region of the Blake-Bahama Outer Ridge. Deep-Sea Res. 18, 145–165.

Barranco, F.T., Balsam, W.L., Deaton, B.C., 1989. Quantitative reassessment of brick red lutites evidence from reflectance spectrophotometry. Mar. Geol. 89, 299–314.

Bianchi, G.G., Vautravers, M., Shackleton, N.J., 2001. Deep flow variability under apparently stable North Atlantic Deep Water production during the last interglacial of the subtropical NW Atlantic. Paleoceanography 16, 307–316.

Bickert, T., Curry, W.B., Wefer, G., 1997. Late Pliocene to Holocene (2.6–0 Ma) western Equatorial Atlantic deep-water circulation: Inferences from benthic stable isotopes. Proc. ODP Sci. Results 154, 239–254.

Blanc, P.L., Rabussier, D., Vergnaud-Grazzini, C., Duplessy, J.C., 1980. North Atlantic deep water formed by the later middle Miocene. Nature 283, 553–555.

Blumsack, S.L., Weatherly, G.L., 1989. Observations of the nearby flow and a model for the growth of mudwaves. Deep-Sea Res. A 36, 1327–1339.

Brew, D.S., Mayer, L.A., 1998. Modelling of Pliocene–Pleistocene abyssal mudwaves using synthetic seismograms. Mar. Geol. 149, 3–16.

Broecker, W.S., 1991. The great ocean conveyor. Oceanography 4, 79–89.

Broecker, W.S., Denton, G.H., 1989. The role of ocean-atmosphere reorganizations in glacial cycles. Geochim. Cosmochim. Acta 53, 2465–2501.

Flood, R.D., 1978. Studies of Deep-Sea Sedimentary Microtopology in the North Atlantic Ocean. Unpublished Doctoral Thesis, WHOI/MIT, Woods Hole, MA.

Flood, R.D., 1980. Deep-sea sedimentary morphology: modeling and interpretation of echo-sounding profiles. Mar. Geol. 38, 77–92.

Flood, R.D., 1988. A lee wave model for deep-sea mudwave activity. Deep-Sea Res. A 35, 973–983.

Flood, R.D., 1994. Abyssal bedforms as indicators of changing bottom current flow – examples from the US east-coast continental rise. Paleoceanography 9, 1049–1060.

Flood, R.D., Hollister, C.D., 1974. Current-controlled topography on the continental margin off the eastern United States In: Burk, C.A., Drake, C.L. (Eds.), The Geology of Continental Margins. Springer-Verlag, Berlin, pp. 197–205.

Flood, R.D., Pirmez, C., Yin, H., 1997. The compressional wave velocity of Amazon Fan sediments: Calculation from index properties and variation with clay content. In: Flood, R.D., Piper, D.J.W., Klaus, A., Peterson, L.C. (Eds.), Proc. ODP Sci. Results 155, 477–493.

Flood, R.D., Shor, A.N., Manley, P.L., 1993. Morphology of abyssal mud waves at Project MUDWAVES sites in the Argentine Basin. Deep-Sea Res. II 40, 859–888.

Giosan, L., Flood, R.D., Grützner, J., Franz, S.-O., Poli, M.-S., Hagen, S., 2001. High-resolution carbonate content estimated from diffuse spectral reflectance for Leg 172 sites. In: Keigwin, L.D., Rio, D., Acton, G.D., Arnold, E. (Eds.), Proc. ODP Sci. Results 172 [Online]. Available from http://www-odp.tamu.edu/publications/172_SR/chap_06/chap_06.htm.

Giosan, L., Flood, R.D., Aller, R.C., 2002a. Paleoceanographic significance of sediment color on western North Atlantic drifts: I. Origin of color. Mar. Geol. 189, 25–41.

Giosan, L., Flood, R.D., Grützner, J., Mudie, P., 2002b. Paleoceanographic significance of sediment color on western North Atlantic drifts: II. Late Pliocene–Pleistocene sedimentation. Mar. Geol. 189, 43–61.

Grützner, J., Giosan, L., Franz, S.-O., Tiedemann, R., Cortijo, E., Chaisson, W.P., Flood, R.D., Hagen, S., Keigwin, L.D., Poli, M.-S., Rio, D., Williams, T., 2002. Astronomical age models for Pleistocene drift sediments from the western North Atlantic (ODP Sites 1055 to 1063). Mar. Geol. 189, 5–23.

Hagelberg, T.K., Shackleton, N., Pisias, N., Shipboard Scientific Party, 1991. Development of composite depth sections for sites 844 through 854, Proc. ODP Init. Rep. 138, 79–85.

Haskell, B.J., 1991. The Influence of Deep Western North Atlantic Circulation on Late Quaternary Sedimentation on the Blake Outer Ridge. PhD Thesis, Duke University, Durham, NC.

Hollister, C.D., Heezen, B.C., 1972. Geologic effects of ocean bottom currents: Western North Atlantic. In: Gordon, A.L. (Ed.), Studies in Physical Oceanography, Gordon and Breach, New York, pp. 37–66.

Hollister, C.D., Flood, R.D., Johnson, D.A., Lonsdale, P.F., Southard, J.B., 1974. Abyssal furrows and hyperbolic echo traces on the Bahama Outer Ridge. Geology 2, 395–400.

Hopfauf, V., Spiess, V., 2001. Fachbereich Geowissenschaften.

A three-dimensional theory for the development and migration of deep sea sedimentary waves. Deep-Sea Res. 48, 2497–2519.

Imbrie, J. et al., 1992. On the structure and origin of major glaciation cycles. 1. Linear responses to Milankovitch forcing. Paleoceanography 7, 701–738.

Imbrie, J., Berger, A., Boyle, E.A., Clemens, S.C., Duffy, A., Howard, W.R., Kukla, G., 1993. On the structure and origin of major glaciation cycles. 2. The 100,000-year cycle. Paleoceanography 8, 699–735.

Jenkins, W.J., Rhines, P.B., 1980. Tritium in the deep North-Atlantic ocean. Nature 286, 877–880.

Johns, E., Fine, R.A., Molinari, R.L., 1997. Deep flow along the western boundary of the Blake Bahama Outer Ridge. J. Phys. Oceanogr. 27, 2187–2208.

Keigwin, L.D., Rio, D., Acton, G., et al., 1998. Proc. ODP Init. Results, 172.

Laughton, A.S., 1981. The first decade of GLORIA. J. Geophys. Res. 86, 11511–11534.

Manley, P.L., Flood, R.D., 1993. Paleoflow history determined from mudwave migration; Argentine Basin. In: Manley, P.L., Flood, R.D. (Eds.), Project Mudwaves. Deep-Sea Res. II 40, 1033–1055.

Mayer, L.A., 1979a. Deep-sea carbonates: acoustical, physical and stratigraphic properties. J. Sediment. Petrol. 47, 1593–1597.

Mayer, L.A., 1979b. The origin of fine-scale acoustic stratigraphy in deep-sea carbonates. J. Geophys. Res. 84, 6177–6184.

McCave, I.N., Swift, S.A., 1976. Physical model for rate of deposition of fine-grained sediments in deep-sea. Geol. Soc. Am. Bull. 87, 541–546.

McCave, I.N., Tucholke, B.E., 1986. Deep current-controlled sedimentation in the western North Atlantic. In: Tucholke, B.E., Vogt, P.R. (Eds.), The Western North Atlantic Region, GSA, The Geology of North America, vol. M, pp. 593–610.

Miller, K.G., Tucholke, B.E., 1983. Development of Cenozoic abyssal circulation south of the Greenland-Scotland Ridge. In: RidgeBott, M.H.P., Saxov, S., Talwani, M., Thiede, J. (Eds.), Structure and Development of the Greenland-Scotland Ridge; New Methods and Concepts. NATO Conf. Ser. IV, Mar. Sci. 8, 549–589.

Normark, W.R., Hess, G.R., Stow, D.A.V., Bowen, A.J., 1980. Sediment waves on the Monterey Fan levees: a preliminary physical interpretation. Mar. Geol. 37, 1–18.

Paillard, D., Labeyrie, L., Yiou, P., 1996. Macintosh program performs time-series analysis. EOS Trans. AGU 77, 379.

Raymo, M.E., Ruddiman, W.F., Shackleton, N.J., Oppo, D.W., 1990. Evolution of Atlantic-Pacific gradients over the last 2.5 m.y. Earth Planet. Sci. Lett. 97, 353–368.

Raymo, M.E., Oppo, D.W., Curry, W., 1997. The mid-Pleistocene climate transition: A deep sea carbon isotopic perspective. Paleoceanography 12, 546–559.

Schmieder, F., von Dobeneck, T., Bleil, U., 2000. The Mid-Pleistocene climate transition as documented in the deep South Atlantic Ocean: initiation, interim state and terminal event. Earth Planet. Sci. Lett. 179, 539–549.

Stahr, F.R., Sanford, T.B., 1999. Transport and bottom boundary layer observations of the North Atlantic Deep Western Boundary Current at the Blake Outer Ridge. Deep-Sea Res. II 46, 205–243.

Tucholke, B.E., 1979. Furrows and focused echoes on the Blake Outer Ridge. Mar. Geol. 31, M13–M21.

Weatherly, G.L., 1993. On deep-current and hydrographic observations from a mudwave region and elsewhere in the Argentine Basin. Deep-Sea Res. II 40, 939–961.

Wynn, R.B., Weaver, P.P.E., Ercilla, G., Stow, D.A.V., Masson, D.G., 2000. Sedimentary processes in the Selvage sediment-wave field, NE Atlantic: new insights into the formation of sediment waves by turbidity currents. Sedimentology 47, 1181–1197.

Zhang, J., 1997. Application of a Model for Mud Wave Evolution. MS Thesis, Marine Sciences Research Center, State University of New York at Stony Brook, Stony Brook, NY, 64 pp.